Impact of Mineralizing Agents on Aluminum Distribution and Acidity of ZSM-5 Zeolites

Shadi Al-Nahari, Eddy Dib, Claudia Cammarano, Etienne Saint-Germes, Dominique Massiot, Vincent Sarou-Kanian, Bruno Alonso

Impact of mineralizing agents on aluminum distribution and acidity of ZSM-5 zeolites

Shadi Al-Nahari,[a] Eddy Dib,[c] Claudia Cammarano,[a] Etienne Saint-Germes,[a] Dominique Massiot,[b] Vincent Sarou-Kanian,[b] Bruno Alonso[a,*]

[a] ICGM, Université de Montpellier, CNRS, ENSCM, 34293 Montpellier cedex 5, France
[b] CNRS, CEMHTI UPR3079, Univ. Orléans, 45071 Orléans cedex 2, France
[c] LCS, Normandie Univ, ENSICAEN, UNICAEN, CNRS, 14000 Caen, France
* bruno.alonso@enscm.fr

ABSTRACT

Intensive research on improving the catalytic properties of zeolites is focused on modulating their acidity and the distribution of associated Al sites. Herein, by studying a series of ZSM-5 zeolites over a broad range of Al content, we demonstrate for the first time that the nature of the mineralizing agent used in hydrothermal syntheses directly impacts Al site distributions. The proportions of Al sites, probed by ^{27}Al NMR, depend on the Si/Al ratio for F^-, but remain identical for OH^- (from Si/Al=30 to 760). This leads to contrasting variations in weak and strong acidities. Such opposite effect of F^- and OH^- mineralizers can be explained by the spatial location of negative charges and the resulting balance between short- and long-range electrostatic interactions. It represents a simple and new opportunity to control zeolites' acidity.

KEYWORDS

Acidity, Electrostatic interactions, Hydrothermal synthesis, NMR spectroscopy, Temperature Programmed Desorption, Zeolites

TABLE OF CONTENTS GRAPHIC

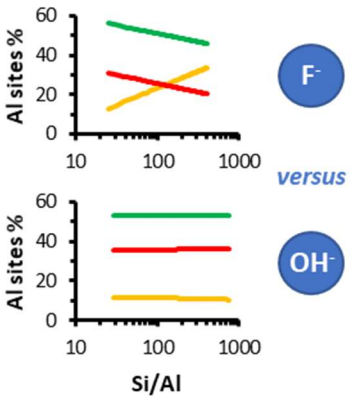

The mineralizing agents F^- and OH^- directly impact aluminum distribution in ZSM-5. Al sites' proportions depend on the Si/Al ratio for F^-, but remain identical for OH^- (from Si/Al = 30 to 760). This opposite effect offers a simple and new opportunity to control zeolites' acidity and further reactivity.

Owing to the crucial role of acidity in heterogeneous catalysis, much effort is devoted to control the reactivity and selectivity of zeolites through the variation of Brønsted acid sites distribution.[1] Acid sites are typically formed when $[AlO_4]^{5-}$ tetrahedra substituting a certain amount of $[SiO_4]^{4-}$ tetrahedra in the zeolite framework are compensated by protons, creating Brønsted sites Si-(OH)-Al. During zeolite formation, the interplay between negative and positive charges in the growing framework has a considerable effect on the zeolite phase selectivity and stability. More specifically, the charge distribution, and the related electrostatic interactions, are expected to determine the distribution of negatively charged aluminium tetrahedra in the frameworks of zeolites. These charges are brought by (i) the forming elements sources (Si, Al), (ii) the organic or inorganic cations acting as structure directing agents (SDAs), and (iii) the mineralizing agents (F^- or OH^-).

In this sense, one of the current strategies to tune Al sites distribution is based on the variations in positively charged SDAs. For instance, this strategy has been proposed for ZSM-5, one of the zeolites widely used in industrial catalytic applications,[2] following different approaches. Al sitting variations can be achieved by tuning the relative proportions of tetrapropylammonium (TPA) - the most efficient organic SDA for this zeolite - and inorganic SDAs such as Na^+,[3] or by replacing, partially or totally, TPA by alcohol and amine molecules[4] or other organic SDAs.[5] The positioning of SDAs' positive charges in the 10 membered ring (MR) channels (e.g. inorganic cations) or at their crossing (e.g. TPA) is thought to direct the positioning of Al at these locations,[3c] although this is a matter of debate.[6] Furthermore, this strategy is shown to improve the efficiency of the catalysts in terms of activity and selectivity.[1c,3c,4a,7]

An alternative strategy, not yet developed, is to exploit the mineralizing agents as a possible mean to tune Brønsted acid sites distribution. When the amount of negatively charged Al tetrahedra in the zeolite is below that of the positive charges brought by the SDAs, the electrical neutrality is insured by negative charges coming from the mineralizing agents employed. Taking the example of the ZSM-5 zeolite, and considering a wide range of Si/Al molar ratio, we demonstrate here how F^- and OH^- anions affect oppositely Al sites distribution.

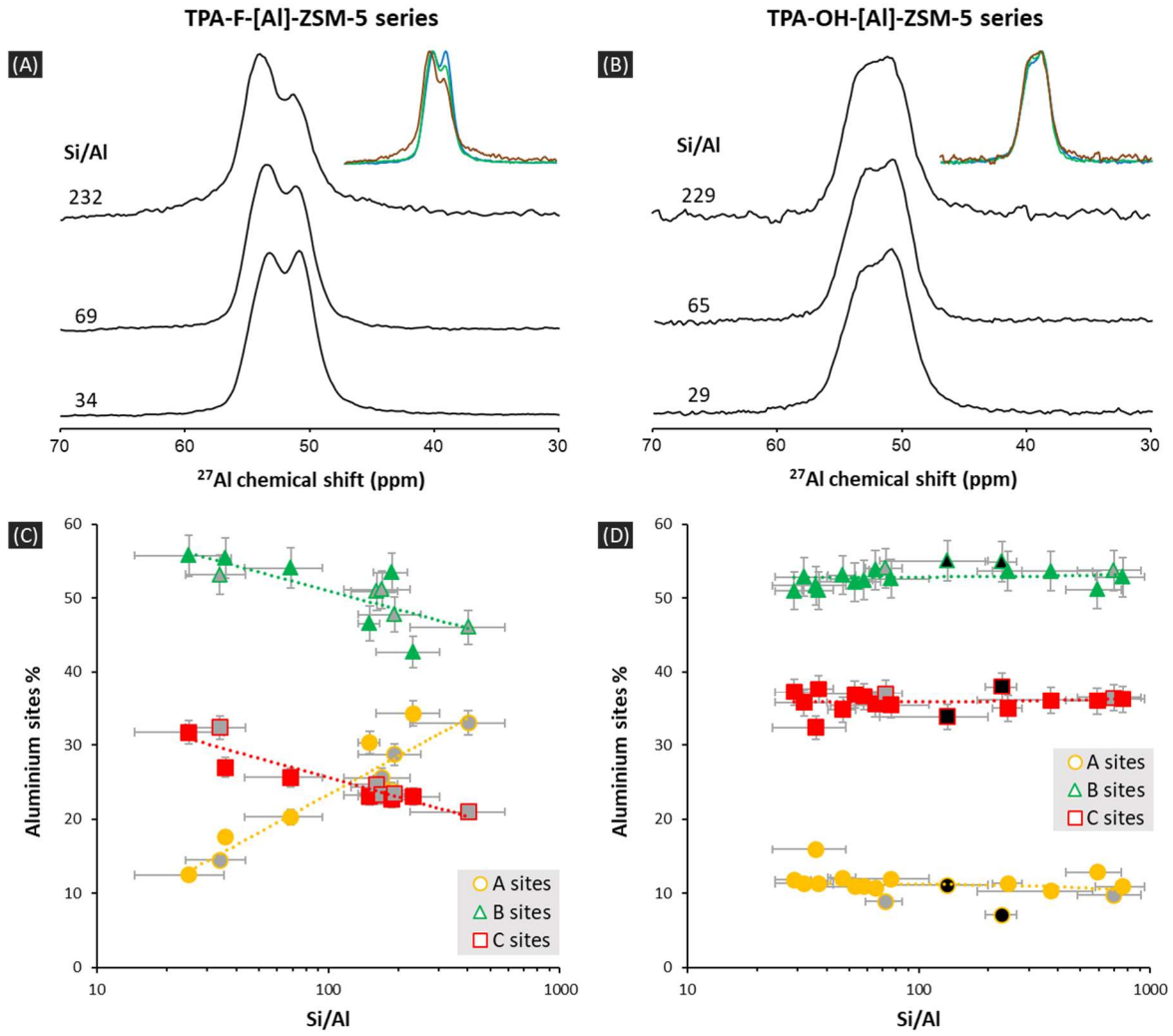

Figure 1. Variations in Al sites distributions probed by ^{27}Al NMR. (A-B) ^{27}Al spectra of TPA-F-[Al]-ZSM-5 (A) and TPA-OH-[Al]-ZSM-5 (B) zeolites obtained with F^- or OH^- anions as mineralizing agents, for three different Si/Al molar ratio (B_0 = 14.1 T, ν_{MAS} = 18 kHz). The onsets present overlapped comparisons. (C-D) Variations of Al sites percentages - A sites (○), B sites (Δ) and C sites (□) - as a function of Si/Al for TPA-F/OH-[Al]-ZSM-5 zeolites. Data is obtained by fitting ^{27}Al NMR spectra recorded at 14.1 T. (A) F^- route: symbols filled in grey correspond to $Al(NO_3)_3.9H_2O$ as Al precursor, others to $Al(OH)_3$. (B) OH^- route: symbols filled in grey correspond to $Al(NO_3)_3.9H_2O$ and TEOS as Al and Si precursors, symbols filled in black to $Al[OCH(CH_3)_2]_3$ and fumed silica precursors, other symbols to $Al[OCH(CH_3)_2]_3$ and TEOS precursors. Dashed lines, obtained through a linear regression, are only guide for eyes.

We chose to synthesize [Al]-ZSM-5 zeolites using TPA as single SDA in order to avoid any concomitant effect of other SDAs (see Supporting Information **SI 1** for details). This choice leads to one positive charge per 24 tetrahedral T sites of the MFI framework of ZSM-5. The lowest reachable Si/Al molar ratio is therefore 23. Close to this ratio, the negative compensating charges coming from the anions are scarce. In this case, ^{27}Al NMR MAS spectra of the as-synthesized TPA-[Al]-ZSM-5 exhibit characteristic peaks of $[Al(OSi)_4]$ units forming a similar envelope whatever the mineralizing anion used (**Figures 1A-B**). When Si/Al increases, ^{27}Al spectra do change when fluoride is used as a mineralizing agent as it was noticed early.[8] On the contrary, and not remarked until now, no real evolution is observed for the hydroxide route (**Figure 1B**). Importantly, the same observations are made for the resulting calcined H-[Al]-ZSM-5 that would be used for catalysis (**Figure S5**). Moreover, for these calcined zeolites, we found interesting trends from temperature programmed desorption of ammonia

(NH_3-TPD). The use of F^- anions as mineralizers, that favors aluminum A sites at high Si/Al, also favors a higher proportion of strong acidity, while the use of OH^- doesn't (**Figure 2**, **Table S6**).

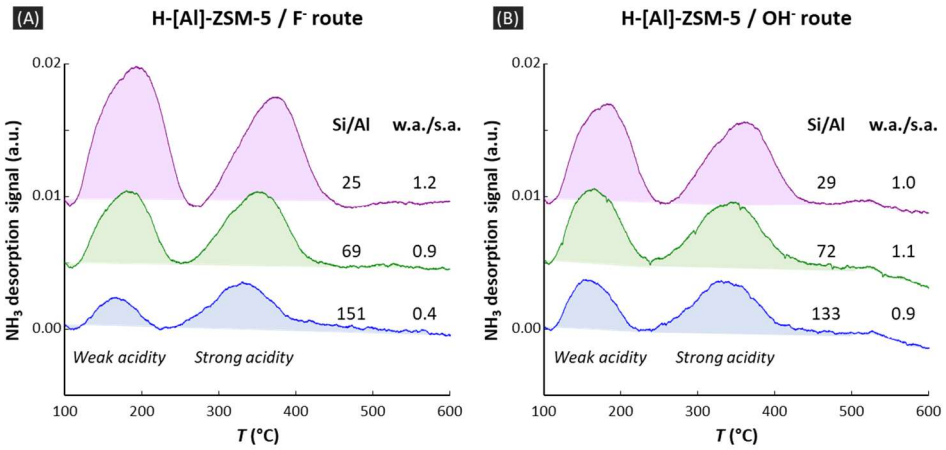

Figure 2. NH_3-TPD thermograms (rate = 10 °C.min^{-1}) of calcined H-[Al]-ZSM-5 zeolites obtained with F^- and OH^- mineralizing agents (A and B respectively). Signal intensities are normalized over sample weight. The ratio w.a./s.a. refers to the ratio between weak and strong acidities expressed as NH_3 concentration. Colors are only used for visualization's purposes.

The differences in ^{27}Al peaks positions for tetrahedrally coordinated Al in $[Al(OSi)_4]$ units are commonly related to differences in SiOAl angles,[9] and thus on Al siting positions. In the case of ZSM-5, the Al sites distribution is not random and some crystallographic sites are preferentially occupied as demonstrated by ^{27}Al NMR.[3a,8] Therefore, the differences observed in 1D spectra are intimately related to differences in Al sites distribution. For a representative selection of TPA-F/OH-[Al]-ZSM-5 zeolites, we have recorded 2D ^{27}Al 3Q-MAS spectra at different magnetic fields (14.1 and 20.0 T). Three ^{27}Al peaks, located at isotropic chemical shifts of 55.5 ppm (A sites), 53.8 ppm (B sites) and 51.4 ppm (C sites), are identified by spectrum fitting (**Tables S7-S8**). They were used for quantifying the Al sites' proportions using a robust 1D fitting procedure (Supporting Information **SI 4**). The variations of these proportions are plotted as a function of Si/Al in **Figure 1C-D** (**Figure S15** for the results obtained at 20.0 T).

At low Si/Al, the percentages of the three ^{27}Al peaks are almost the same (± 5 %) for both mineralizing agents: ca. 10, 55 and 35 % for the A, B and C sites respectively. In the case of F^- anions, there are important and gradual variations in sites' percentages. A sites are promoted to ca. 35 % at the expenses of the other B and C sites when increasing Si/Al, and thus the F content, in line with previous observations.[8,10] Noteworthy changes in the Al precursors, $Al(OH)_3$ or $Al(NO_3)_3$, or in the initial amount of water (**Table S1**) do not modify the observed trend (**Figure 1D**). In the case of OH^-, an opposite behavior is observed, with no significant variation in sites' percentages over the wide Si/Al range explored. Furthermore, the chemical variations made in the synthesis's protocol (Si and Al precursors, initial H_2O/Si molar ratio), that do change crystal sizes (**Figure S2**), do not influence this result.

A possible explanation for these contrasted behaviors can be found in the relative location of charges within the zeolite framework. Positive charges are brought by the TPA cations at the crossing between channels in the MFI structure (one per 24 Si). Negative charges arise from Al insertion, and when Si/Al is above 23, from F^- anions or silanolates SiO^- groups depending on the mineralizing agent used, F^- or OH^- respectively. The silanolates are in interaction with silanol groups forming nests with a characteristic ^1H peak located at ca. 10 ppm.[11] For the ZSM-5 zeolites studied here, the relative signal

area of this peak decreases consistently when Al content increases (**Figure S16**). It was previously shown that these silanol nests are spatially close to H_γ (methyl groups of TPA).[12] In experimental or DFT optimized crystal structures,[13] H_γ atoms are close to all T sites (distances between 2.8 and 4.5 Å), which is not the case for H_β and H_α atoms (methylene groups). This allows therefore various possibilities for the location of the silanolate groups leading to a high degree of local disorder probed by ^{29}Si and ^{14}N NMR for as-synthesized silicalite-1 obtained with the OH^- route.[14] Surprisingly, this distribution of silanolates in ZSM-5 is not altering the Al sites distribution - which does not prevent the formation of Al pairs at low Si/Al [4b],[15] - whatever the initial gel composition. On the contrary, despite the preservation of the specific location of F^- within the $[4^15^26^2]$ cage close to the 4 MR of the MFI framework at variable Si/Al,[16],[10] the Al sites distribution is altered. This specific location might therefore be the reason of changing the Al distribution and favoring A sites.

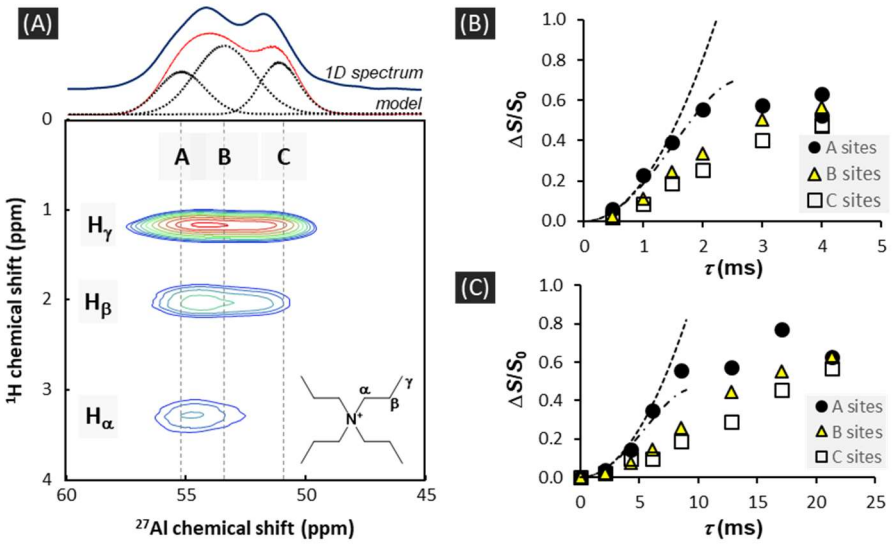

Figure 3. Al-TPA spatial proximities. (A) $^1H\{^{27}Al\}$ *D*-HMQC of a TPA-F-[Al]-ZSM-5 zeolite (Si/Al = 30, $T \approx 300$ K, B_0 = 20.0 T, ν_{MAS} = 100 kHz). The spectrum is transposed for an easier comparison. (B) $^{27}Al\{^1H\}$ REDOR plots of TPA-F-[Al]-ZSM-5 zeolite with selective H_α pulses (Si/Al = 30, $T \approx 300$ K, B_0 = 20.0 T, ν_{MAS} = 100 kHz). (C) $^{27}Al\{^{31}P\}$ REDOR plots of an as-synthesized zeolite obtained using TPP and a F^- route (Si/Al = 25, $T \approx 243$ K, B_0 = 14.1 T, ν_{MAS} = 15 kHz). The dotted lines correspond to the REDOR curves for spin pairs with first and second order approximation[17] that better model the initial build-ups for A sites.

Spatial proximities between Al sites and TPA cations can be inferred from NMR experiments based on dipolar couplings. The improvement in ^1H resolution using very high magnetic field (20.0 T) and MAS frequencies (100 kHz) renders possible to clearly distinguish the TPA's peaks (H_α, H_β and H_γ). $^1H\{^{27}Al\}$ D-HMQC correlation spectra (**Figure 3A**) and $^{27}Al\{^1H\}$ REDOR experiments (**Figure 3B** and **S17**, **Table S9**), with ^1H selective π refocusing pulses irradiating only one type of ^1H resonance, demonstrate that H_α are spatially closer to Al in A sites (< 3.5 Å) than in B and C sites (≤ 4.0 Å) while H_β and H_γ are at similar distances to all Al sites. And this remains valid for both F^- and OH^- routes (**Figure S6**). Besides, we verified that similar $^{27}Al\{^1H\}$ REDOR spectra with H_α selection are obtained for a TPA-F-[Al]-ZSM-5 zeolites with contrasted Al contents (Si/Al = 30 or 232) (**Figure S18**, **Table S10**). We also conducted a $^{27}Al\{^{31}P\}$ REDOR analysis on ZSM-5 zeolite synthesized using tetrapropylphosphonium (TPP) instead of TPA, and a F^- route. The sample presents the same ^{27}Al spectrum as the related sample obtained with TPA at same Si/Al (**Figure S8**). The resulting ^{27}Al-^{31}P dipolar couplings can give then a good indication for the Al-N distances in standard TPA-F/OH-[Al]-ZSM-5 samples. The $^{27}Al\{^{31}P\}$ REDOR curves, recorded at low *T* (≈243 K) to decrease the effect of motions, show a faster build-up for A sites (**Figure 3C**). This

confirms the closer proximity of A sites to the center of the OSDA, with here Al-P distances estimated around 4.8 Å (**Table S9**). If we refer to TPA-[Al]-ZSM-5 structures refined from X-rays diffraction data, this distance is the smallest that can be found for Al-N, and corresponds to tetrahedral sites T1 (d_{AlN} = 5.0 Å, *Pnma* space group)[18] or T13 (d_{AlN} = 4.9 Å, $Pn2_1a$ space group).[19] These T sites are located at the crossing between pore channels and bound to the 4 MR of the MFI framework, thus close to [$4^1 5^2 6^2$] cages. Such possible siting positions for A sites are consistent with a previous assignment made on the basis of DFT calculations.[20] It is to note that T1/T13 sites belong to the preferential locations for Al in ZSM-5 often reported.[3a,19-21] Other short Al-N distances (d_{AlN} < 5.3 Å) correspond to T sites in the [$4^1 5^2 6^2$] cages. In the case of B and C sites, the Al-P distances are between 5.5 and 5.7 Å (**Table S9**). In the TPA-[Al]-ZSM-5 structures, the related Al-N distances correspond to T sites that are located in the channels or at their crossing, usually far from the [$4^1 5^2 6^2$] cages.

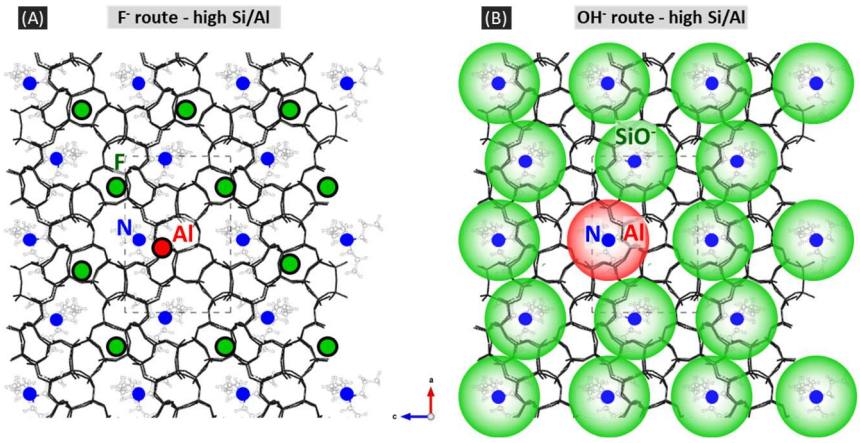

Figure 4. Schematic visualization of the distributions of the positive charges coming from TPA (represented as point charges at N positions, blue circles), the negative charges brought by the mineralizing anions F^- and OH^-, and the favored sitting positions of Al in ZSM-5 zeolites at high Si/Al. (A) F^- route: F atoms (green dots) are located in the [$4^1 5^2 6^2$] cages, favored Al atom is sitting at the T1 site (red dot), close to N and to the crystallographic position of F. (B) OH^- route: silanolates are distributed around TPA (SiO^-, green spheres), Al atoms can be located in large areas (red sphere). The black lines represent the SiO bonds of the silica MFI framework projected onto the ac plane.

The above results can be understood by considering a balance between short- and long-range interactions. Preferential Al siting positions can be defined by strong short-range interactions between negatively charged framework areas and positively charged OSDA. This determines a distribution of Al sites that is identical at Si/Al close to 23 (one Al per OSDA) whatever the mineralizing anions. For higher Si/Al values, the other negative compensating charges might tune or not the Al distribution. The presence of F^- at single defined crystal positions certainly modify the long-range electrostatic interactions. The Al sites that most minimize the energy of these interactions are then more favored. They correspond here to Al in A sites close to the crystallographic positions of F (**Figure 4A**). On the contrary the distribution of silanolates over different crystallographic sites doesn't affect significantly long-range interactions, and the Al sites distribution does not vary over a wide range of Si/Al ratio (30 to 760).

This opposite effect of mineralizing anions on Al sites distribution sheds lights on the importance of considering the spatial distribution of all negative charges within the zeolite frameworks when discussing Al sitting modulation. It also opens new and simple means to control and tune the distribution of Brønsted acid sites and the acidity of zeolites, notably for high Si/Al ratios, and further their catalytic properties.

ACKNOWLEDGEMENTS

The French National Research Agency (ANR) is acknowledged for funding this research through the project ZEOORG ANR-19-CE29-0008-01. The French research facility Infranalytics (FR-2054) is acknowledged for the access to a high magnetic field (20 T). We gratefully thank Franck Fayon, Pierre Florian and Philippe Gaveau for their stimulating discussions and help in solid-state NMR experiments. Gérard Delahay and Christine Biolley are acknowledged for their ideas and implication in TPD analyses.

REFERENCES

[1] a) J. Dedecek, Z. Sobalik, B. Wichterlova, *Catal. Rev.* **2012**, *54*, 135-223; b) B. C. Knott, C.T. Nimlos, D. J. Robichaud, M. R. Nimlos, S. Kim, R. Gounder, *ACS Catal.* **2018**, *8*, 770-784; c) T. T. Le, A. Chawla, J. D. Rimer, *J. Catal.* **2020**, *391*, 56-68.

[2] a) B. Yilmaz, U. Müller, *Top. Catal.* **2009**, *52*, 888-895; b) C. Martínez, A. Corma, *Coord. Chem. Rev.* **2011**, *255*, 1558-1580.

[3] a) S. Sklenak, J. Dedecek, C. B. Li, B. Wichterlova, V. Gabova, M. Sierka, J. Sauer, *Angew. Chem. Int. Ed.* **2007**, *46*, 7286-7289; b) J. Dedecek, V. Balgová, V. Pashkova, P. Klein, B. Wichterlová, *Chem. Mater.* **2012**, *24*, 3231-3239; c) T. Yokoi, H. Mochizuki, S. Namba, J. N. Kondo, T. Tatsumi, *J. Phys. Chem. C* **2015**, *119*, 15303-15315.

[4] a) T. Yokoi, H. Mochizuki, T. Biligetu, Y. Wang, T. Tatsumi, *Chem. Lett.* **2017**, *46*, 798-800; b) C. T. Nimlos, A. J. Hoffman, Y. G. Hur, B. J. Lee, J.R. DiIorio, D. D. Hibbitts, R. Gounder, *Chem. Mater.* **2020**, *32*, 9277-9298.

[5] A. Chawla, R. Li, R. Jain, R. J. Clark, J. G. Sutjianto, J. C. Palmer, J. D. Rimer, *Mol. Syst. Des. Eng.* **2018**, *3*, 159-170.

[6] V. Pashkova, S. Sklenak, P. Klein, M. Urbanova, J. Dědeček, *Chem. Eur. J.* **2016**, *22*, 3937-3941.

[7] a) T. Biligetu, Y. Wang, T. Nishitoba, R. Otomo, S. Park, H. Mochizuki, J. N. Kondo, T. Tatsumi, T. Yokoi, *J. Catal.* **2017**, *353*, 1-10; b) H. Liu, H. Wang, A. H. Xing, J. H. Cheng, *J. Phys. Chem. C* **2019**, *123*, 15637-15647.

[8] O. H. Han, C. S. Kim, S. B. Hong, *Angew. Chem. Int. Ed.* **2002**, *41*, 469-472.

[9] E. Lippmaa, A. Samoson, M. Magi, *J. Am. Chem. Soc.* **1986**, *108*, 1730-1735.

[10] E. Dib, T. Mineva, P. Gaveau, E. Véron, V. Sarou-Kanian, F. Fayon, B. Alonso, *J. Phys. Chem. C* **2017**, *121*, 15831-15841.

[11] H. Koller, R. F. Lobo, S. L. Burkett, M. E. Davis, *J. Phys. Chem.* **1995**, *99*, 12588-12596.

[12] E. Dib, J. Grand, S. Mintova, C. Fernandez, *Chem. Mater.* **2015**, *27*, 7577-7579.

[13] a) T. Mineva, E. Dib, A. Gaje, H. Petitjean, J.-L. Bantignies, B. Alonso, *ChemPhysChem* **2020**, *21*, 149 –153; b) M. Fabbiani, S. Al-Nahari, L. Piveteau, E. Dib, V. Veremeienko, A. Gaje, D. G. Dumitrescu, P. Gaveau, T. Mineva, D. Massiot, A. van der Lee, J. Haines, B. Alonso, *Chem. Mater.* **2022**, *34*, 366-387.

[14] E. Dib, T. Mineva, P. Gaveau, B. Alonso, *Phys. Chem. Chem. Phys.* **2013**, *15*, 18349-18352.

[15] J. Dědeček, D. Kaucký, B. Wichterlová, *Chem. Commun.* **2001**, 970-971.

[16] C. A. Fyfe, D. H. Brouwer, A. R. Lewis, J. M. Chezeau, *J. Am. Chem. Soc.* **2001**, *123*, 6882-6891.

[17] M. Bertmer, H. Eckert, *Solid State Nucl. Magn. Reson.* **1999**, *15*, 139-152.

[18] H. van Koningsveld, H. van Bekkum, J. C. Jansen, *Acta Cryst. B* **1987**, *43*, 127-132.

[19] Y. Yokomori, S. Idaka, *Microporous Mesoporous Mater.* **1999**, *28*, 405-413.

[20] E. Dib, T. Mineva, E. Véron, V. Sarou-Kanian, F. Fayon, B. Alonso, *J. Phys. Chem. Lett.* **2018**, *9*, 19-24.

[21] a) J. Holzinger, P. Beato, L. Fahl Lundegaard, J. Skibsted, *J. Phys. Chem. C* **2018**, *122*, 15595-15613; b) N. Zhang, C. L. Liu, J. H. Ma, R. F. Li, H. J. Jiao, *Phys. Chem. Chem. Phys.* **2019**, *21*, 18758-18768; c) E. Salvadori, E. Fusco, M. Chiesa, *J. Phys. Chem. Lett.* **2022**, *13*, 1283-1289.